JOURNAL OF CATALYSIS 140, 344–352 (1993)

Investigations of Active Sites for Methane Activation in the Oxidative Coupling Reaction over Pure and Li-Promoted MgO Catalysts

MING-CHENG WU, CHARLES M. TRUONG, KENT COULTER, AND D. WAYNE GOODMAN[1]

Department of Chemistry, Texas A&M University, College Station, Texas 77843-3255

Received May 18, 1992; revised November 9, 1992

The oxidative coupling of methane to ethane over model MgO catalysts prepared under well-controlled, ultrahigh vacuum (UHV) conditions has been studied using a combination of surface science techniques and elevated-pressure kinetic measurements. The utilization of electron energy loss spectroscopy has allowed us to characterize a variety of defects and to identify the active sites which are responsible for the methane coupling reaction. The results indicate that [Li^+O^-] centers are not likely directly involved in the methane activation step, but rather promote the production of F-type centers in the near-surface region which are responsible for this key step in the methane coupling reaction. The origin of [Li^+O^-] and F-type defects and their densities and stabilities are discussed. © 1993 Academic Press, Inc.

I. INTRODUCTION

The oxidative coupling of methane to ethane over alkali metal promoted alkaline earth oxide catalysts has recently received considerable attention due to its technological and fundamental importance. So far, a variety of metal oxides promoted with alkali-metal-containing compounds have been reported to exhibit the enhanced activity for C_2 production (*1*), though C_2 yields, which vary from 14.8 to 23.9% (*2*), are not particularly encouraging at the present time for commercial utilization of such a process. The early work of Lunsford and co-workers (*3–5*) has indicated that the primary activation step of methane occurs at the catalyst surface, yielding methyl radicals. For Li-doped MgO catalysts, it has been suggested that [Li^+O^-] centers, generated by the substitution of Li^+ for Mg^{2+} in the magnesium oxide lattice, are responsible for abstracting hydrogen from methane (*2–5*). The methane reacts with these centers in the following manner:

$$[Li^+O^-] + CH_4 \rightarrow OH_s^- + CH_3.$$

The original Li-containing centers are regenerated by the recombination of two OH_s^- to form water and the reoxidation of the center.

Although there remains some controversy regarding the extent to which this reaction involves an O_s^- center, the concept that the [Li^+O^-] center is directly responsible for methane activation has become widely accepted (*6–9*). However, Matsuura and co-workers (*10, 11*) have recently shown that a 3 mol% Li-promoted MgO catalyst, which gave a C_2 yield of 21.5% at 973 K, exhibited a prominent photoluminescence feature at ~450 nm that was attributed to surface sites of low coordination. The intensity of this photoluminescence feature was observed to parallel the methane coupling activity of the Li/MgO catalyst. Further studies using transmission electron microscopy showed that these ultrafine crystalline magnesium oxide catalysts transformed into spherical-shaped particles upon doping with lithium, indicating exposure of (111) planes instead of the usual (100) planes. The authors therefore concluded that the role of the lithium is to promote the formation of unsaturated or reactive sites on the surface of MgO.

[1] To whom correspondence should be addressed.

0021-9517/93 $5.00

Hutchings and co-workers (*12*) have examined the relationship between catalyst morphology and performance in the methane coupling reaction over MgO catalysts using transmission electron microscopy. It was concluded that the edge and corner sites of MgO particles are not catalytically significant, and the active sites are likely located on the (100) plane of MgO. Addition of lithium into magnesium oxide increased the production of emergent line defects as well as point defects (color centers of either F or V type). These defects may play a significant role in methane activation.

In this article, we present a study of the partial oxidation of methane to ethane over a model MgO catalyst prepared under well-controlled, ultrahigh vacuum (UHV) conditions using a combination of surface science techniques and elevated-pressure kinetic measurements. The results indicate that $[Li^+O^-]$ centers are not likely directly involved in the methane activation step, but rather promote the production of color centers in the near-surface region which are considered to be responsible for this key step in the methane coupling reaction.

II. EXPERIMENTS

The studies were carried out in two UHV systems. The kinetic data was acquired in a combined elevated-pressure reactor/UHV surface analysis chamber equipped with Auger electron spectroscopy (AES) and temperature-programmed desorption (TPD). A separate UHV system containing high-resolution electron energy loss spectroscopy (HREELS) was employed to investigate the electronic transitions associated with a variety of defects. This second UHV system also has capabilities for AES, low energy electron diffraction (LEED) and TPD, and for sample heating and cooling.

The preparation of pure and Li-doped MgO films consists of depositing Mg and codepositing Mg and Li, respectively, onto Mo(100) in a controlled oxygen atmosphere and annealing in an oxygen ambient following the film synthesis. Magnesium deposition was performed via thermal evaporation of a high-purity ribbon tightly wrapped around a tungsten filament. Lithium atoms were deposited onto the surface from a SAES GETTERS source. The two metal dosers were mounted close together inside a cylindrical tantalum cage located approximately 3 cm away from the specimen during metal deposition. A piece of tantalum sheet was used to separate the two dosers in order to eliminate cross-contamination during metal evaporation. The flux of Mg and Li evaporation was directly monitored by a mass spectrometer which was mounted in line with the metal sources. The evaporation rate of the metal vapor was determined by a combination of TPD and AES measurements which has been detailed elsewhere (*13*).

For pure MgO films, our LEED and surface spectroscopic studies (*13*) have shown that the MgO films, prepared under optimum oxidation conditions, grow epitaxially on Mo(100) in the 200–600 K substrate temperature range and have essentially a one-to-one stoichiometry.

Li-promoted MgO films were synthesized under UHV conditions by codepositing Mg and Li onto a clean Mo(100) surface at a substrate temperature of 300 K in 2×10^{-7} Torr of oxygen. Film stoichiometry was adjusted by tuning the relative evaporation flux of Mg and Li. The surface structure studies using LEED have indicated the rock salt lattice of MgO is preserved upon doping with lithium at concentrations ranging from 0–15 at%.

Figure 1 shows some typical Auger spectra acquired following the synthesis of the films. The spectrum of a pure MgO film exhibits two prominent features at 32.0 and 505.0 eV which arise from the $Mg^{2+}(L_{23}VV)$ and $O^{2-}(KLL)$ Auger transitions (*13–16*), respectively. Upon doping with 10 at% Li (see spectrum b), the intensity of the $Mg^{2+}(L_{23}VV)$ Auger transition decreases relative to the $O^{2-}(KLL)$ Auger transition. Spectrum c displays Auger features of an ~10-ML LiO_2 film.

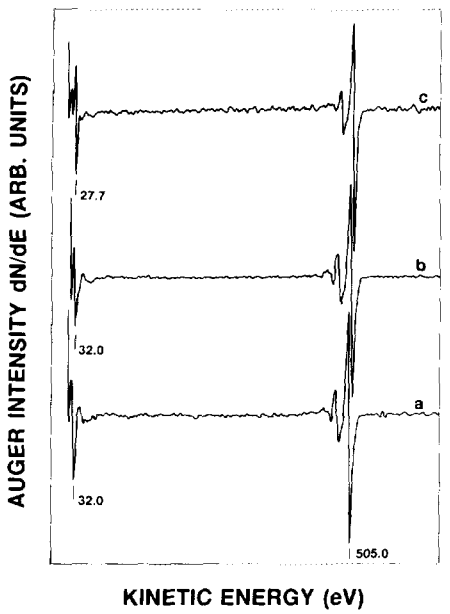

FIG. 1. Auger spectra obtained from (a) a pure MgO film, ~20 monolayers; (b) a 10 at% Li-doped MgO film, ~20 monolayers; and (c) a pure Li_2O film, ~10 monolayers.

Upon completion of film preparation and characterization in the spectroscopic chamber, the model catalyst was transferred in situ into the reaction chamber through a double-stage differentially pumped teflon sliding seal. The reaction was then carried out at 990 K in 6 Torr of reactants with an $O_2:CH_4$ ratio of 1:5. After a 5-min reaction, the product gas mixture was analyzed with gas chromatography utilizing a flame ionization detector. The details of these experiments including a comparison of activities and activation energies between the Li/MgO films and Li/MgO powders of Lunsford and co-workers (*3–5*) are described elsewhere (*17*).

The HREELS measurements were carried out in the scattering compartment of a two-tiered chamber (*18*). The primary energy of the electron beam of the spectrometer (LK-2000, Larry Kesmodel Technologies) can be varied in the 0–250 eV range. The HREELS instrument is operated routinely at an energy resolution (full-width at half maximum of the elastic peak) of 5–10 meV. However, in order to maximize the loss intensities which are often several orders of magnitude smaller than the elastic peak, the spectra were acquired at an energy resolution of 30 meV. An elastic-peak count rate of 10^6 Hz was easily obtained with this energy resolution.

III. RESULTS

Figure 2a presents the ethane production measured at 990 K as a function of sample pretreatment temperature, T. The oxide films were pretreated by heating in oxygen

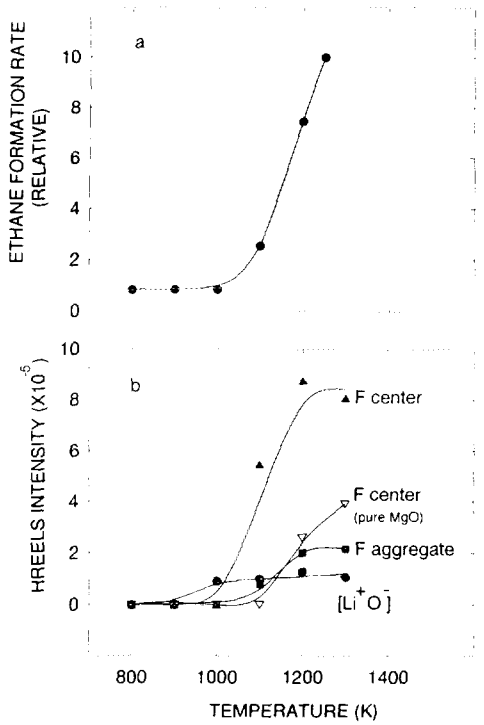

FIG. 2. (a) Ethane formation rate measured as a function of sample pretreatment temperature. The reaction was carried out at a sample temperature of 990 K for 5 min and with a partial pressure of CH_4 and O_2 of 5 and 1 Torr, respectively. The Li/MgO films were grown on Pt(100) for the kinetic measurements. The Li loading was approximately 10 at%. (b) HREELS intensities of the various defects normalized to the respective elastic peak versus the sample pretreatment temperature. Open symbols represent the data obtained from pure MgO films. The Li content was 10 at%.

to various temperatures (700–1300 K) prior to reaction. A 10-fold increase in the ethane yield at 990 K is apparent as the pretreatment temperature of the catalyst is increased from 1000 to 1250 K. Figure 3 gives Arrhenius plots obtained from the turnover frequency of ethane formation versus the inverse reaction temperature. The apparent activation energies for pure and 10 at% Li-promoted MgO films are deduced to be 60 and 50 kcal/mol, respectively.

Model thin films prepared in the same manner as those used in the kinetic experiments were characterized in the HREELS system. Figure 4 presents a set of HREELS spectra acquired from ~20-monolayer MgO films as a function of sample pretreatment temperature. The spectra obtained from pure MgO films exhibit a prominent loss feature at 6.3 eV. This feature is believed to be due to a surface-related interband transition associated with surface atoms of five-fold coordination (*19*) since its energy is considerably less than the 7.8 band gap of MgO (*20*). No loss feature is observed in the 0–5 eV spectral region, except for the sharp peaks which occur in the region very

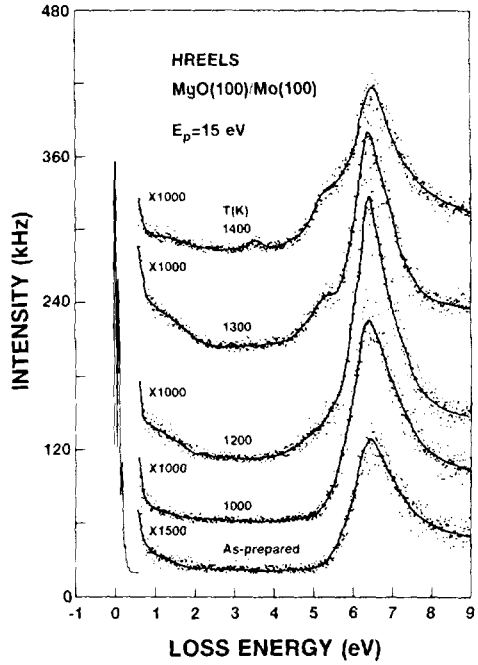

FIG. 4. HREELS spectra of an ~20 monolayer MgO film on Mo(100) acquired subsequent to annealing in 5×10^{-7} Torr of oxygen for 1 min to the temperatures indicated. The films were prepared at a substrate temperature of 300 K, and the data were collected in the specular direction using an electron beam with E_p = 15 eV at a substrate temperature of 80 K.

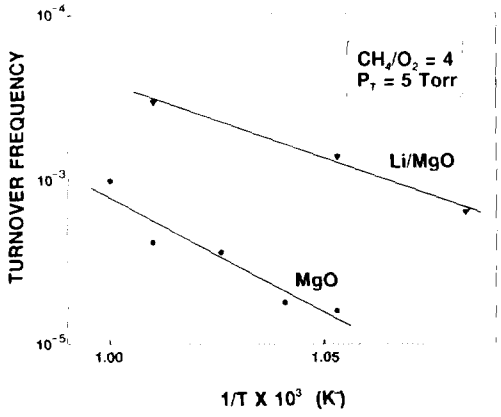

FIG. 3. The Arrhenius plots of turnover frequency versus inverse reaction temperature. The Li-promoted MgO films were grown on Pt(100) for the kinetic measurements. The apparent activation energies for pure and 10 at% Li-promoted MgO films of 60 and 50 kcal/mol, respectively, are approximately the same within experimental error.

near the elastic peak. These features originate from losses due to the excitation of the surface optical phonon and multiples thereof.

Upon annealing to ≥1200 K, three loss features emerge in the bulk band gap region of MgO, as shown in Fig. 4. Detailed studies regarding identification and characterization of these features are described elsewhere (*21*). The loss features observed at 1.1, 3.6, and 5.3 eV have been attributed to surface F centers (surface oxygen vacancies containing two electrons), F aggregates, and F centers (near-surface oxygen vacancies containing two electrons), respectively (*21–24*). These intrinsic defects of MgO are thermally generated only in the 1200–1400 K temperature range. From the HREELS and TPD studies (*21*), we have

concluded that the MgO films synthesized on a Mo(100) surface are thermally stable and nearly free from defects up to 1100 K, above which defects in MgO films are generated. At $T \simeq 1400$ K, a significant portion of the MgO films has desorbed as indicated in our HREELS and TPD spectra (*21*). The desorption of MgO films is complete at temperatures above ~1500 K.

Thin films prepared by codepositing Mg and Li onto a clean Mo(100) surface in an oxygen environment have been characterized using HREELS. Figure 5 presents a set of HREELS spectra acquired subsequent to heating the films to various temperatuures, followed by a rapid cooling to 80 K. The as-prepared films containing 10 at% lithium exhibit HREELS spectra which are very similar to those of pure MgO films. Upon annealing to $T \geq 1000$ K, a distinct loss feature at ~1.6 eV emerges and saturates in intensity with an increase in annealing temperature. Two additional loss features at 3.6 and 5.3 eV develop at $T \geq 1100$ K. These latter features have the same loss energies as those found for pure MgO films and are thus attributed to F aggregates and F centers. Further studies including the electron beam energy dependence of these features indicate that the species giving rise to these excitations are in the near-surface region (several monolayers below the topmost 1–2 layers of the film) (*21*). In Fig. 2b, the intensities of these losses, together with those obtained from the pure MgO films, are normalized to the respective elastic peak and plotted as a function of annealing temperature.

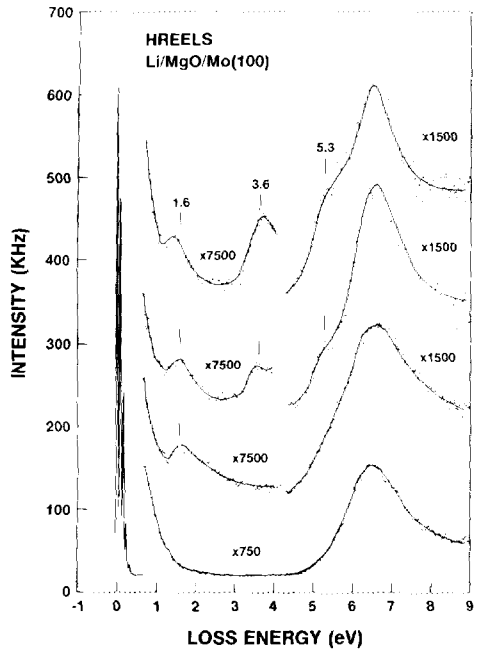

FIG. 5. HREELS spectra acquired subsequent to heating a 10 at% Li-doped MgO film on Mo(100) in 5×10^{-7} Torr of oxygen to various temperatures, followed by a rapid cooling to 80 K: (a) as-prepared at 300 K, (b) 1000 K, (c) 1100 K, and (d) 1200 K. The film thickness is 20 monolayers. The loss features marked at 1.6, 3.6, and 5.3 eV in the figure are attributed to $[L^+O^-]$ centers, F aggregates, and F centers, respectively. The spectral data were collected using an electron beam with a primary energy of 15 eV at a sample temperature of 80 K.

The evolution of defect features observed in HREELS has also been examined as film stoichiometry is varied, as shown in Fig. 6. The pure MgO films exhibit no loss features within the bulk band gap region following an anneal to $T = 1100$ K, whereas three distinct peaks at 1.6, 3.6, and 5.3 eV occur upon annealing the Li-doped MgO films to $T \geq 1100$ K. The intensities of these loss features are dependent on the Li concentration. Included in Fig. 6e is the spectrum of a pure Li_2O film which shows a loss peak at 5.6 eV.

The centers of the type $[M^+O^-]$ in single crystals of alkaline earth oxides have been previously studied by Abraham and coworkers (*25–29*) using electron spin resonance (ESR) and optical absorption spectroscopy. These authors have shown that the production of the $[Li^+O^-]$ centers gives rise to a characteristic resonance at $g_\perp = 2.054$ and $g_\parallel = 2.0043$ in ESR spectra, and to a characteristic feature which maximizes at 1.8 eV in the optical absorption spectrum. The loss feature observed at ~1.6 eV therefore indicates the presence of $[Li^+O^-]$ centers in the near-surface region in our MgO films.

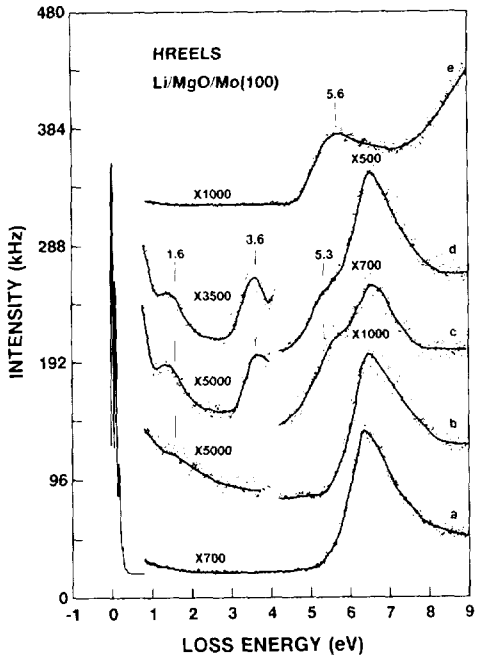

FIG. 6. HREELS spectra versus the Li concentration: (a) a pure MgO film, T = 1000 K; (b) a 1.7 at% Li-doped MgO film, T = 1000 K; (b) a 1.7 at% Li-doped MgO film, T = 1200 K; (c) a 10 at% Li-doped MgO film, T = 1200 K; (d) a 15 at% Li-doped MgO film, T = 1200 K; and (e) a pure Li_2O film, as prepared at 300 K. The film thickness is 20 monolayers. The spectral data were collected using an electron beam with a primary energy of 15 eV at a substrate temperature of 80 K.

IV. DISCUSSION

The conclusion that $[Li^+O^-]$ centers are directly responsible for methane activation has been derived primarily from experiments in which the number of methyl radicals formed (*4*) and the rate of ethane formation (*5*) were found to parallel the density of $[Li^+O^-]$ centers as the Li concentration was varied. The present studies, however, show that for a particular Li concentration (10 at%), the $[Li^+O^-]$ HREELS intensity remains essentially constant in the 1000–1300 K temperature region, whereas a 10-fold increase is observed in the ethane yield. This behavior thus is contrary to the assumption that $[Li^+O^-]$ centers play a direct role in the methane activation step. On the other hand, it is found that the concentration of F centers (F aggregates) and the ethane production change in concert, as shown in Fig. 2, consistent with the F centers being directly responsible for the methane activation step. It follows then that the generation of methyl radicals occurs via surface F centers, namely, surface sites of low coordination. These surface sites are assumed to be in equilibrium with bulk F centers and F aggregates at the high temperatures typically used for this reaction. The presence of Li in MgO apparently increases the production of F-type defects, an increase that is likely a consequence of the substitution of Li^+ for Mg^{2+} in the magnesium oxide lattice.

This promotion is evident in Fig. 6, in which the concentration of F defects in MgO at a particular sample pretreatment temperature is found to increase with an increase in the Li content. Furthermore, Fig. 2b clearly shows the difference between promoted and unpromoted MgO films in the production of F centers. The density of F defects at T = 1200 K, for example, is approximately fourfold greater in the promoted films than in the unpromoted films. From the above discussion, it is also clear that although the $[Li^+O^-]$ concentration increases with an increase in the Li content, this increase can not account for the increase in the ethane production. Instead, the enhanced activities of Li-promoted MgO catalysts for ethane production is a consequence of the increase in the density of F centers and F aggregates in the near-surface region which occurs following the addition of Li to MgO.

Further support for our argument that F centers rather than $[Li^+O^-]$ centers are the key reaction sites is that pure and Li-promoted MgO exhibit approximately the same apparent activation energies for ethane formation, as shown in Fig. 3. This feature implies that the methane activation occurs via active sites of the same type over pure and Li-promoted MgO films because different sites very likely would give rise to different activation energies. The 10-fold

increase in ethane production is explained by an increase in the number of active sites on the surface during the reaction.

The argument for the F center being the active site is also consistent with the fact that the maximum density of F-type defects is much greater than that of $[Li^+O^-]$ defects. In early ESR and optical absorption studies (*30, 31*), the concentration of F^+ defects in MgO was found to saturate at a level of $\sim 10^{19}$ cm^{-3} during neutron irradiation. The formation of vacancy aggregates was suggested to be responsible for this maximum density (*30, 31*). The concentration of the $[Li^+O^-]$ defects which arise following the addition of Li into MgO, on the other hand, was reported to be on the order of 10^{16}–10^{17} cm^{-3} (*2, 6*), which is approximately 1 ppm of the oxygen ions in MgO. These centers have been found to be present largely in the bulk with small surface concentrations (*6*).

In the present studies, the F defect HREELS intensity increases as T is increased from 1000–1200 K and saturates at $T \geq 1200$ K, as shown in Fig. 2b. This behavior, along with the appearance of F aggregates, suggests that the maximum density of F defects in our MgO films is obtained at the annealing temperature above 1200 K. That is, the Li-promoted MgO films after high-temperature treatment contain F defects at approximately 10^{19} cm^{-3}, which is estimated from the saturation density reported in literature (*30, 31*). Assuming the cross sections of the F defect and the $[Li^+O^-]$ defect for electron excitation are on the same order of magnitude, the obtained HREELS intensity ratio of the F center to the $[Li^+O^-]$ center of $\sim 10:1$ is consistent with the above estimation in that the maximum density of F-type defects greatly exceeds that of $[Li^+O^-]$ defects.

The $[Li^+O^-]$ defect in many aspects resembles the V^- center which possesses a cation vacancy with a hole trapped in an adjacent lattice oxygen ion. From the catalytic point of view both the centers can be regarded as an O^- center. Indeed, previous optical absorption studies indicated that the production of the $[Li^+O^-]$ defect gives rise to an absorption band with a maximum at 1.8 eV (*25–29*) which is near the absorption maximum of the V^- center (2.3 eV) (*32*), but far away from the absorption maximum of the F/F^+ center (5.0 eV) (*30, 31*). Both the $[Li^+O^-]$ and V^- centers were reported to be highly unstable and can be readily bleached thermally and optically (*25–29, 32*), whereas the F-type center exhibits high thermal stability (*24, 30, 31*). In the absence of multivalent transition metal ion impurities, such unstable defects of the O^- type can not be produced in MgO because the excessive charge in the centers has to be compensated by the impurities in order to maintain the charge neutrality in the sample. The density of these unstable centers thus depends strongly on the content of the impurities.

In as-grown Li/MgO crystals, the density of the unstable $[Li^+O^-]$ centers was, in fact, reported to be negligibly small (*26–28*). However, a sizable concentration of $[Li^+O^-]$ defects can be obtained by high-temperature or electron irradiation treatment of the specimen (*26–28*). According to the model of Abraham and co-workers (*26*), the lithium impurities in as-grown MgO crystals are considered to concentrate primarily in precipitates (probably in the oxide form of Li_2O) with some soluble Li^+ ions randomly distributed in the crystal. These soluble Li^+ ions give rise to the unstable $[Li^+O^-]$ center. Upon high-temperature or extensive electron irradiation treatment, each precipitate generates a microgalaxy of substitutional Li^+ ions surrounding the precipitate, giving rise to a cloud of the stable $[Li^+O^-]$ centers. Charge neutrality within the microgalaxy requires that Li^+ ions are predominantly in the $[Li^+O^-]$ state.

It then follows from the above model that for every two Li^+ leaving the Li_2O precipitate due to thermal diffusion, only one Mg^{2+} cation enters to form MgO. From stoichiometric considerations, the lack of oxygen ions in the crystal can result in the forma-

tion of oxygen vacancies, i.e., F centers. This is indeed the case in the present studies and in the work of Abraham and coworkers (*26–28*) in which the production of F-type centers was found to increase with an increase in the Li content.

The studies of pure MgO films have demonstrated that the generation of F-type defects occurs in the 1200–1400 K temperature range. In Li-doped MgO films, F defects may be produced via an additional route, i.e., the thermal desorption of Li_2O precipitates at high temperatures, which results in the formation of vacancies in the bulk of MgO. Our thermal desorption studies have shown that pure Li_2O films desorb above 1000 K with a maximum at ~1250 K. It then follows that the desorption of Li_2O results in a decrease in the production of the stable $[Li^+O^-]$ centers, whereas the remaining precipitates produces more $[Li^+O^-]$ centers due to enhanced thermal diffusion of Li^+ at higher temperatures. This competition process may explain why the $[Li^+O^-]$ HREELS intensity remains essentially constant over the 1000–1300 K temperature range. In any of the cases discussed above the production of F defects is favored.

In summary, based on the following evidence, the F defects are proposed to be responsible for the methane activation step in the coupling reaction: (1) parallel correlation between the density of F defects rather than that of $[Li^+O^-]$ centers and the ethane formation rate with respect to the sample pretreatment temperature; (2) approximately the same apparent activation energies for methane activation over pure and Li-promoted MgO films; and (3) thermal stability and maximum density considerations of F defects versus $[Li^+O^-]$ defects.

V. CONCLUSIONS

In conclusion, the oxidative coupling of methane to ethane over a model MgO catalyst prepared under well-controlled, UHV conditions have been studied using combined surface science techniques/elevated-pressure kinetic measurements. The utilization of electron energy loss spectroscopy in conjunction with elevated-pressure kinetic measurements has allowed us to characterize a variety of defects and to identify possible active sites which might be responsible for the methane coupling reaction. The results indicate that $[Li^+O^-]$ centers are not likely directly involved in the methane activation step, but rather promote the production of F-type centers in the near-surface region which are responsible for this key step in the methane coupling reaction. The origin of $[Li^+O^-]$ centers and F centers has been discussed, and a comparison of their maximum densities has been made.

ACKNOWLEDGMENTS

We acknowledge with pleasure the support of this work by the Gas Research Institute and the Department of Energy, Office of Basic Energy Sciences, Division of Chemical Science.

REFERENCES

1. Hutchings, G. J., Scurrel, M. S., and Woodhouse, J. R., *Chem. Soc. Rev.* **18,** 251 (1989).
2. Lunsford, J. H., *Catal. Today* **6,** 235 (1990).
3. Ito, T., and Lunsford, J. H., *Nature (London)* **314,** 721 (1985).
4. Driscoll, D. J., Martir, W. Wang, J.-X., and Lunsford, J. H., *J. Am. Chem. Soc.* **107,** 58 (1985).
5. Ito, T., Wang, J.-X., Lin, C.-H., and Lunsford, J. H., *J. Am. Chem. Soc.* **107,** 5062 (1985).
6. Wang, J.-X., and Lunsford, J. H., *J. Phys. Chem.* **90,** 5883 (1986).
7. Lee, J. S., and Oyama, S. T., *Catal. Rev.-Sci. Eng.* **30,** 249 (1988).
8. Anderson, J. R., *Appl. Catal.* **47,** 177 (1989).
9. Peng, X. D., Richards, D., and Stair, P. C., *J. Catal.* **121,** 99 (1990).
10. Matsuura, I., Utsumi, Y., Doi, T., and Yoshida, Y., *Appl. Catal.* **47,** 299 (1989).
11. Anpo, M., Sunamoto, M., Doi, T., and Matsuura, I., *Chem. Lett.* 701 (1988).
12. Hargreaves, J. S. J., Hutchings, G. J., Joyner, R. W., and Kiely, C. J., *J. Catal.*, in press.
13. Wu, M.-C., Corneille, J. S., Estrada, C. A., He, J.-W., and Goodman, D. W., *Chem. Phys. Lett.* **182,** 472 (1991).
14. Namba, H, Darville, J., and Gilles, J. M., *Surf. Sci.* **108,** 446 (1981).
15. Bermudez, V. M., and Ritz, V. H., *Surf. Sci.* **82,** L601 (1979).

16. Flodström, S. A., and Martinsson, C. W. B., *Surf. Sci.* **118,** 513 (1982).
17. Coulter, K., and Goodman, D. W., *Catal. Lett.* **6,** 191 (1992).
18. Wu, M.-C., Estrada, C. A., Corneille, J. S., and Goodman, D. W., *J. Chem. Phys.*, in press.
19. Henrich, V. E., Dresselhaus, G., and Zeiger, H. J., *Phys. Rev. B* **22,** 4764 (1980).
20. Roessler, D. M., Walker, W. C., *Phys. Rev.* **159,** 733 (1967).
21. Wu, M.-C., Truong, C. M., and Goodman, D. W., *Phys. Rev. B* **46,** 12688 (1992).
22. Weber, H., *Z. Phys.* **30,** 392 (1951).
23. Hensley, H. B., and Kroes, R. L., *Bull. Am. Phys. Soc.* **13,** 420 (1986).
24. Henderson, B., and Wertz, J. E., "Defects in the Alkaline Earth Oxides." Taylor & Francis LDT, London, 1977.
25. Abraham, M. M., Chen, Y., Boatner, L. A., and Reynolds, R. W., *Phys. Rev. Lett.* **37,** 849 (1976).
26. Chen, Y., Tohver, H. T., Narayan, J., and Abraham, M. M., *Phys. Rev. B* **16,** 5535 (1977).
27. Lacy, J. B., Abraham, M. M., Boldu, J. L., Chen, Y., Narayan, J., and Tohver, H. T., *Phys. Rev. B* **18,** 4136 (1978).
28. Boldu, J. L., Abraham, M. M., and Chen, Y., *Phys. Rev. B* **19,** 4421 (1979).
29. Olson, D. N., Orera, V. M., Chen, Y., and Abraham, M. M., *Phys. Rev. B* **21,** 1258 (1980).
30. Henderson, B., and King, R. D., *Philos. Mag.* **13,** 1149 (1966).
31. Henderson, B., and Bowen, D. H., *J. Phys. C: Solid State Phys.* **4,** 1487 (1971).
32. Abraham, M. M., Chen, Y., and Unruh, W. P., *Phys. Rev. B* **9,** 1842 (1974).